

Journal of Materials Chemistry B

Accepted Manuscript



This is an *Accepted Manuscript*, which has been through the Royal Society of Chemistry peer review process and has been accepted for publication.

Accepted Manuscripts are published online shortly after acceptance, before technical editing, formatting and proof reading. Using this free service, authors can make their results available to the community, in citable form, before we publish the edited article. We will replace this *Accepted Manuscript* with the edited and formatted *Advance Article* as soon as it is available.

You can find more information about *Accepted Manuscripts* in the [Information for Authors](#).

Please note that technical editing may introduce minor changes to the text and/or graphics, which may alter content. The journal's standard [Terms & Conditions](#) and the [Ethical guidelines](#) still apply. In no event shall the Royal Society of Chemistry be held responsible for any errors or omissions in this *Accepted Manuscript* or any consequences arising from the use of any information it contains.

1 *Regular article*

2

3 **Swim bladder collagen forms hydrogel with macroscopic superstructure by**
4 **diffusion induced fast gelation**

5

6

7 Md. Tariful Islam Mredha^a, Xi Zhang^b, Takayuki Nonoyama^c, Tasuku Nakajima^c, Takayuki
8 Kurokawa^c, Yasuaki Takagi^d and Jian Ping Gong^{c*}

9

10 ^a*Graduate School of Life Science, Hokkaido University, Sapporo 060-0810, Japan*

11 ^b*Graduate School of Fisheries Sciences, Hokkaido University, Hakodate 041-8611, Japan*

12 ^c*Faculty of Advanced Life Science, Hokkaido University, Sapporo 060-0810, Japan*

13 ^d*Faculty of Fisheries Sciences, Hokkaido University, Hakodate 041-8611, Japan*

14

15

16

17

18

19

20

21

22 **Corresponding author*

23 *E-mail: gong@mail.sci.hokudai.ac.jp (J.P.G); Tel & FAX: +81-(0)11-706-2774*

24

25

26 **ABSTRACT:** Marine collagen has been attracting attention as medical materials in recent
27 times due to the low risk of pathogen infection compared to animal collagen. Type I collagen
28 extracted from swim bladder of Bester sturgeon fish has excellent characteristics such as high
29 denaturation temperature, high solubility, low viscosity and extremely fast rate to form large
30 bundle of fiber at certain conditions. These specific characteristics of swim bladder collagen
31 (SBC) permit us to create stable, disk shaped hydrogels with concentric orientation of
32 collagen fiber by the controlled diffusion of neutral buffer through collagen solution at room
33 temperature. However, traditionally used animal collagens, e.g. calf skin collagen (CSC) and
34 porcine skin collagen (PSC) could not form any stable and oriented structure by this method.
35 The mechanism of superstructure formation of SBC by diffusion induced gelation process has
36 been explored. The fast fibrillogenesis rate of SBC causes a quick squeezing out of solvent
37 from the gel phase to the sol phase during gelation, which builds an internal stress at the gel-
38 sol interface. The tensile stress induces the collagen molecules of gel phase to align along the
39 gel-sol interface direction to give this concentric ring-shaped orientation pattern. On the other
40 hand, the slow fibrillogenesis rate of animal collagens due to the high viscosity of the
41 solution does not favor the ordered structure formation. The denaturation temperature of SBC
42 increases significantly from 31°C to 43°C after gelation, whereas that of CSC and PSC was
43 found to increase a little. Rheology experiment shows that SBC gel has storage modulus
44 larger than 15 kPa. The SBC hydrogels with thermal and mechanical stability have potentials
45 as bio-materials for tissue engineering applications.

46

47

48 *Key words:* Hydrogel, swim bladder collagen, superstructure, diffusion, denaturation
49 temperature.

50

51 1. INTRODUCTION

52 Hydrogels, a class of soft and wet material, are considered to be the most promising smart
53 bio-materials due to their similarity to soft bio-tissues. Developments of hydrogels in last
54 decade¹⁻⁵ greatly enhanced the applications of this material in various fields, including
55 artificial organs, drug delivery, regenerative medicine etc.⁶⁻⁹ Collagen-based hydrogels for
56 biomedical application are becoming very hot topic in medical research because of their low
57 antigenic activity, high cell adhesion properties, biocompatibility, and biodegradability.^{10,11}
58 Numerous specific functions of many bio-tissues are strongly dependent on the anisotropic
59 superstructure of fiber-forming collagen.^{12,13} The most common sources of collagen for
60 biomaterials and tissue engineering are bovine skin and tendons, porcine skin, and rat tail.¹¹
61 In recent times, the use of collagen and collagen-derived products from land-based animal
62 calls into question because of the emergence of zoonosis such as bovine spongiform
63 encephalopathy (BSE), foot-and-mouth disease (FMD), avian influenza diseases etc.^{14,15}
64 Religious beliefs also restrict the usage of porcine or bovine collagens. Marine resource has
65 been attracting attention at the very recent times as a smart alternative of animal collagen due
66 to their low risk of pathogen infection and no religious obstruction.¹⁶

67

68 A huge source of marine-based collagen is now from the wastes of seafood industry.
69 Recently, Zhang *et al.*¹⁷ have found that the swim bladder of Bester sturgeon fish (a hybrid
70 sturgeon of *Husohuso* x *Acipenserruthenus*) is a large source of type I collagen (18.1% on a
71 wet weight basis, 37.7% on a dry weight basis), which has relatively high thermal stability
72 (32.9°C by CD spectroscopy). In addition, apart from the conventional animal collagen, this
73 swim bladder collagen (SBC) has excellent characteristics such as high solubility and
74 homogeneity, low viscosity and extremely fast rate to form large bundle of fiber at certain
75 conditions. However, collagens from other tissues (scales, skin, muscle, digestive tract,

76 notochord and snout cartilage) of Bester sturgeon do not show those interesting properties.¹⁷
77 Until now, hydrogels from marine-based collagen have hardly been developed because of the
78 poor availability in comparison with the land-based animal collagen that is abundant in the
79 market.^{18,19} Being a marine sourced atelocollagen, SBC is expected to have low antigenicity
80 with less risk of pathogen infection and thus, would be suitable for medical application.¹⁶
81 However, the immunostimulant characteristics may not always depend only on the terminal
82 group, the removal of telopeptide group would be preferable to make a biomaterial with
83 relatively better safety profile.^{20,21} In this work, we focus on developing collagen hydrogels
84 with ordered structure by utilizing this marine sourced type I atelocollagen that has the
85 distinguished properties.

86
87 Many efforts have been made for creating ordered structure in collagen-based materials by
88 various methods, including dialysis, shear, hydrodynamic flow, electric field, electro-
89 spinning and magnetic field techniques.²²⁻²⁹ In this work, we use the diffusion-induced
90 gelation to prepare SBC hydrogels. It is well-known that negatively charged polyelectrolytes
91 having rigid nature, such as DNA, alginate, and poly(2,2'-disulfonyl-4,4'-benzidine
92 terephthalamide) (PBDT) form physical hydrogels when Ca^{2+} ions are allowed to diffuse into
93 these polymer solutions.³⁰⁻³⁷ Furthermore, these rigid molecules after gelation are orientated
94 perpendicular to the diffusion direction of Ca^{2+} ion.³⁴⁻³⁷ This specific superstructure formation
95 during diffusion-induced gelation has been related to the syneresis effect of gelation.³⁷ That is,
96 the complexation of negatively charged rigid macromolecules with Ca^{2+} leads to gelation,
97 which induces shrinkage of the gel phase. Since the sol phase does not shrink, an internal
98 stress is built at the sol-gel interface, where the sol phase exerts a tension to the gel phase and
99 the gel phase exerts a compression to the sol phase. As a result, the macromolecules in the gel
100 phase orient along the tensile direction. Our previous study also revealed that, when we

101 develop programmed swelling mismatch in different regions of a hydrogel containing semi-
102 rigid macromolecules, the mismatch induced internal stress determine the orientation of
103 macromolecules in respective regions.⁵

104

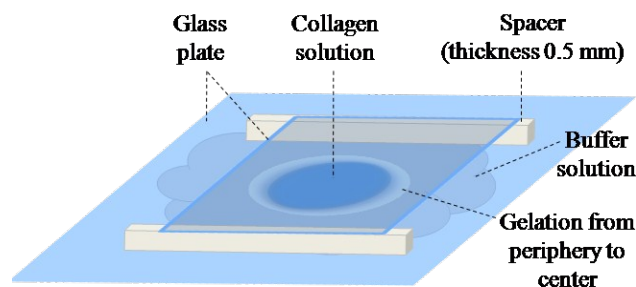
105 Although different rigid macromolecules are successfully oriented by diffusion induced
106 gelation process, but still now, it remains a challenge to make oriented structure in collagen
107 hydrogel due to some limitations of animal collagen. In this work, we intend to develop
108 collagen hydrogels with ordered structure based on this mechanism by utilizing the
109 distinguished properties of SBC. Previous study has clarified that SBC molecules are in
110 stable triple-helix molecular form in acidic solution, and they self-assemble into fibrils in
111 neutral buffer.¹⁷ This is because in acidic solution the collagen is positively charged and in
112 the neutral buffer, it becomes almost neutral, which favors fibril formation.^{38,39} Thus, if we
113 perform controlled diffusion of neutral buffer into acidic SBC solution, we expect super
114 structure formation of SBC molecule by quick fibrillogenesis of the rigid SBC molecule.

115

116 2. EXPERIMENTAL SECTION

117 **Materials:** Type I collagen (atelocollagen) was extracted from the swim bladder of Bester
118 sturgeon fish according to the previously reported protocol.¹⁷ The swim bladder collagen was
119 denoted as SBC. Type I calf skin collagen, CSC (tropocollagen, Sigma Aldrich, Japan) and
120 Type I porcine skin collagen, PSC (atelocollagen, Nippi Co. Ltd.) were used as received
121 without further purifications. Analytical grade Na_2HPO_4 and NaH_2PO_4 (Wako Pure Chemical
122 Industries Ltd., Japan) were used as received for the preparations of Na-phosphate buffer
123 solution of pH 7.2. Concentrated HCl (Wako Pure Chemical Industries Ltd., Japan) was used
124 to prepare aqueous HCl solution of pH 2.5 for the preparation of collagen solutions. All the
125 aqueous solutions were prepared using ultrapure deionized water.

126 **Diffusion induced gelation process:** To prepare collagen solution, a prescribed amount of
127 collagen was dissolved in *aq.* HCl (pH 2.5). The mixture was left for 3 days without any
128 external perturbations at room temperature (25°C) to get a homogenous solution. After that, a
129 drop (~20 μ L) of collagen solution was placed on a glass plate and covered by another glass
130 plate with a gap distance of 0.5 mm, which was controlled by two silicone spacer, as shown
131 in Figure 1. The disk-shaped collagen solution was in contact with the glass plates with an
132 initial diameter about ~6 mm. Gelation of collagen was performed by introducing 0.1 M Na-
133 phosphate buffer (pH 7.2) into the reaction cell from the peripheral part of collagen solution.
134 Gelation progressed from periphery to center of the collagen solution by the diffusion of
135 buffer. After 2 hours, disk shaped collagen hydrogel with diameter ~6 mm and thickness 0.5
136 mm was formed. For rheological study, we have prepared collagen gel of thickness 1 mm. All
137 the SBC gels were prepared at room temperature (25°C). However; CSC and PSC gels were
138 prepared at 25°C and 34°C. To prepare CSC and PSC gels at 34°C, the collagen and buffer
139 solutions were pre-incubated at that temperature for 10 minutes before starting gelation.



140
141 **Figure 1** Set up for the diffusion induced gelation process of collagen solution. The diameter
142 of the disc-shaped collagen solution was about 6 mm.

143 **Characterization:**

144 **Structure**

145 Time dependent structural change during gelation was monitored under the polarizing optical
146 microscope, POM (Nikon, LV100POL). A color sensitized 530 nm tint plate was used to
147 distinguish collagen orientation. The birefringence at different regions of hydrogel was

148 measured quantitatively from the retardation values using a Berek compensator in POM.
149 Scanning electron microscopy (SEM) (JSM-6010LA, JEOL Ltd.) was applied to study the
150 morphology and orientation of collagen fibril. To prepare the sample for SEM observation,
151 the samples were fixed by 0.1 % (v/v) *aq.* glutaraldehyde for 24 hours and freeze-dried using
152 a freeze drying device (Advantage XL-70, VirTis freeze-dryer) and finally, coated with gold
153 using an ion-sputtering device (E-1010, Hitachi, Japan). The shape of the sample did not
154 change after freeze drying.

155 **Fibrillogenesis**

156 Fibrillogenesis rate of collagen was studied by monitoring the turbidity change of an equal
157 volume mixture of 0.3 wt % collagen and 0.1 M Na-phosphate buffer (pH 7.2) at 320 nm
158 using a quartz cell of 1 cm path length in UV spectrophotometer (UV-1800, Shimadzu UV
159 Spectrophotometer).

160 **Solution properties**

161 Transparency of collagen solution was determined from the turbidity measurement at 320
162 nm. The dynamic viscosity of collagen solution was measured at 25°C using rheometer
163 (ARES-100FRT) by strain controlled steady rate sweep test with a cone and plate geometry
164 of 25 mm diameter, 0.054 mm gap distance and 0.04 radians cone angle, covering a shear rate
165 ranges from 0.1 s⁻¹ to 10 s⁻¹.

166 **Thermal stability**

167 The denaturation temperature of collagen solution and collagen hydrogel was determined by
168 differential scanning calorimetry, DSC (SII X-DSC7000, SII Nanotechnology Inc.).

169 **Mechanical property**

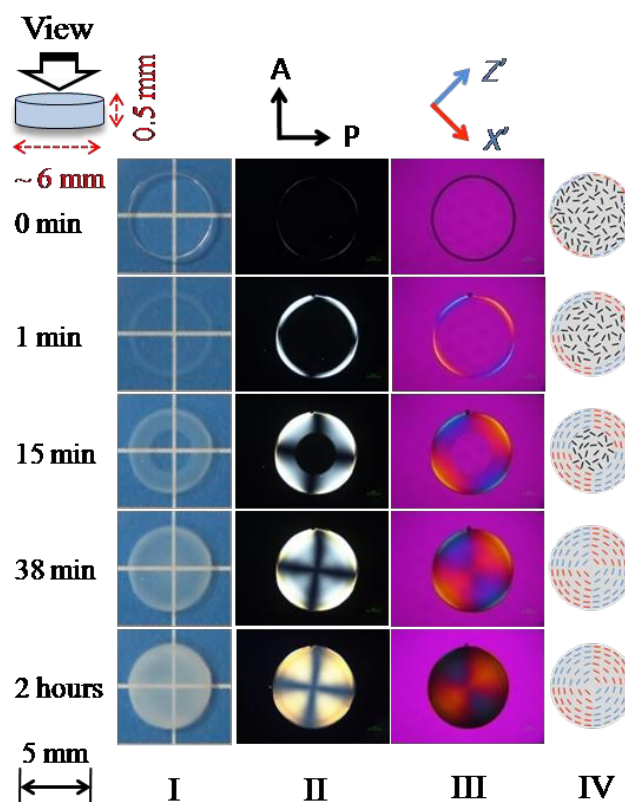
170 To study the mechanical strength of SBC hydrogel, a dynamic frequency sweep test was
171 performed from 0.25 s⁻¹ to 100 s⁻¹ with a shear strain of 0.2 % in the parallel plate geometry

172 at 25°C. A disk shaped SBC gel of thickness 1 mm and diameter 6 mm was adhered to the
 173 plates using glue for measurement.

174

175 3. RESULTS AND DISCUSSION

176 When 0.1 M Na-phosphate buffer solution (pH 7.2) was introduced into the periphery of 4
 177 wt% SBC solution, gelation started immediately from the peripheral part of collagen solution,
 178 which could be confirmed from the turbidity appearance as shown in Figure 2(I). Gelation
 179 continued to progress from the outside to the inside as the buffer solution slowly diffused into
 180 the collagen solution.



181

182 **Figure 2** (I) Photographic images of 4 wt% SBC hydrogel at different gelation time. (II, III)
 183 POM images under crossed polarizer in absence (II) and presence (III) of color sensitized 530
 184 nm tint plate. All the images are in same scale as shown in the bottom left part. (IV)
 185 Illustrations of orientation structure of SBC identified by POM. A: analyzer, P: polarizer. X'
 186 and Z': fast and slow axes of tint plate, respectively.

187 To confirm the presence of oriented structure, we observed the time lapse of gelation
188 processes under POM using crossed polarizer (Figure 2(II)). Before the addition of buffer, no
189 birefringence was observed except at the periphery of collagen solution, indicating that the 4
190 wt% SBC solution is isotropic, well below the liquid crystalline (LC) concentration. This is in
191 consistent with the result by M.M. Giraud-Guille *et al.*,⁴⁰⁻⁴¹ who found that the LC phase of
192 the type I rat tail collagen appears at critical concentration of 8~8.5 wt% in 0.5 M acetic acid
193 (pH 2.5). The peripheral circular birefringence is considered as the edge effect of
194 concentrated polymer solution. The collagen molecules of rigid triple helix assembled at the
195 edge of liquid-air interface to show this ring shaped thin birefringence.

196

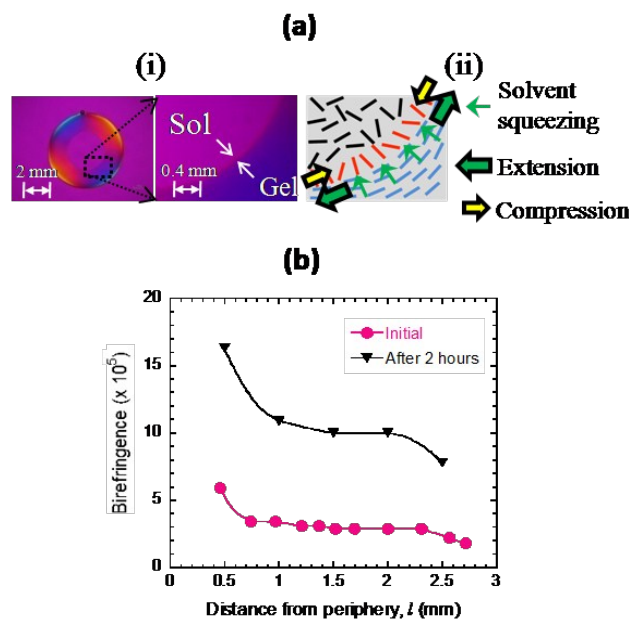
197 The cross patterned of strong birefringence were observed as the gelation progressed from the
198 periphery to center (Figure 2(II)), which indicates the formation of radially or concentrically
199 oriented structure during the diffusion induced gelation process. To confirm the orientation
200 direction, we used color sensitized 530 nm tint plate during POM observation. Denoting that
201 collagen has a positive birefringence⁴², the alternative ring shaped blue (quadrants 2 and 4)
202 and orange (quadrants 1 and 3) colors in POM images (Figure 2(III)) indicate that the
203 collagen molecules orient along and perpendicular to the tint polymer direction, respectively.
204 That is, the collagen is oriented concentrically in the birefringence ring (Figure 2(IV)), in
205 similar to previously reported results on other rigid molecules.³⁷ When the gelation reached
206 the center of the sample at 38 minutes, the concentric orientation was developed in the whole
207 sample. Rigid triple helix collagen molecules have positive charges at acidic condition.³⁸
208 Once the collagen molecules meet with the neutral buffer at the diffusion front, they form
209 aggregated fibers by neutralization. The *syneresis* effect during fiber formation process is
210 considered to be responsible for this super structure formation, in similar to previously
211 reported mechanism.⁵ The fibrillogenesis process causes solvent transportation

212 microscopically, and thus a swelling mismatch is built at the sol/gel interface which insists
213 ordered structure formation. It should be mentioned that the volume change of the gel by
214 contraction during gelation is difficult to observe at macroscopic scale. This is probably due
215 to relatively strong adhesion of the collagen gel to the glass wall of the reaction chamber,
216 which prevents the overall volume change of the gel.

217

218 The *syneresis* induced swelling mismatch can be justified when we observe the gelation front
219 line *in situ* very carefully. A thin line of orange color (indicated by white arrow) ahead of the
220 blue color can be identified at the diffusion front of sol-gel interface (Figure 3(a)(i)). This
221 indicates the presence of radial orientation of collagen ahead of the gelation front as
222 illustrated in Figure 3(a)(ii), which gradually converted into concentric orientation and
223 stabilized with time by forming fiber. During fibrillogenesis process, the contracting gel
224 phase experiences a tensile stress from the very adjacent sol phase. Oppositely, sol phase
225 experiences a compressive stress from the contracting gel phase. Those opposite forces create
226 the concentric and radial orientation in the gel phase and sol-gel boundary, respectively
227 (Figure 3(a)(ii)).

228



229

230 **Figure 3 (a)** POM image (i) of the diffusion/gelation front region under magnified lens and
 231 the corresponding schematic representation (ii) of orientation structure of SBC identified by
 232 POM. **(b)** The birefringence of 4 wt% SBC gel at the position right behind the advancing
 233 gelation front which corresponds to the initially formed structure (denoted as initial in the
 234 Figure) and after 2 hours gelation vs. distance from periphery to center, l .

235

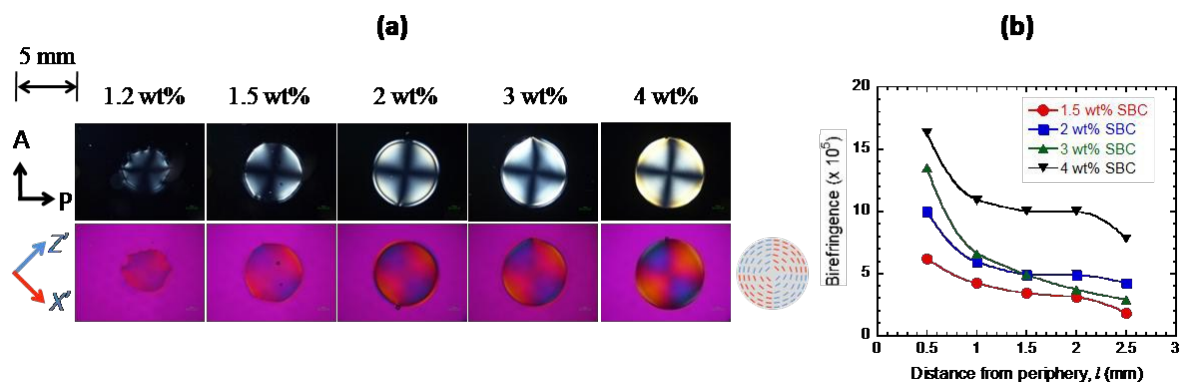
236 The birefringence increases with time. The initial birefringence right behind the gelation front,
 237 which means the structure newly formed with the progress of the diffusion front, is shown in
 238 Figure 3(b). The birefringence obtained after 2 hours gelation is about ~ 3 times higher than
 239 the initial birefringence. The turbidity of the gel also increases drastically during this process
 240 (Figure 2(I)). This observation suggests that fibrillogenesis process continues for the longer
 241 period of time until they reach their characteristic fiber size.

242

243 To understand the effect of collagen concentration on superstructure formation, we have
 244 prepared hydrogel from low to high concentrations of SBC (1.2 ~ 4 wt%). At 1.2 wt% SBC,
 245 the hydrogel only showed weak and irregular birefringence (Figure 4(a)). From 1.5 wt%,

246 distinct cross-patterns were observed, indicating the formation of concentric structure.
247 Therefore, the minimum concentration of SBC required to form a well oriented gel is around
248 1.5 wt%. In addition, at 1.5 wt%~3 wt%, but not at 4 wt%, a thin radially oriented layer can
249 be noticed at the peripheral region (at the boundary of the gel and the buffer). As the viscosity
250 of 1.5 ~ 3 wt% is lower than 4 wt%, this may make it possible for a little outflow of collagen
251 solution at the periphery by the strong diffusion of buffer, which creates this radial
252 orientation at the outer part of hydrogel.

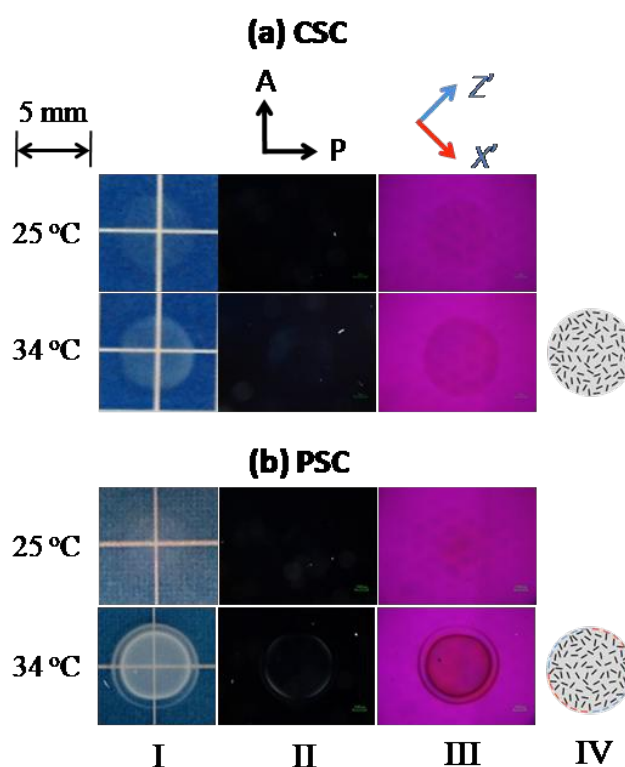
253
254 It could be observed from Figure 4(a) that the birefringence brightness changes with the
255 concentrations of SBC. The brightness of periphery of hydrogel is stronger than that of the
256 center. The birefringence variation with the distance from periphery to center (l) of SBC
257 hydrogels of various concentrations is shown in Figure 4(b). For all the concentrations of
258 SBC, the birefringence decreases with l , which indicates that a gradient of orientation degree
259 is created by the diffusion induced gelation process. Up to ~1 mm distance, birefringence
260 decreases sharply. This is because that the diffusion velocity of buffer sharply decreases at
261 the beginning as the gel width increases and therefore, the rate of fibrillogenesis also
262 decreases. So the swelling mismatch created from *syneresis effect* also decreases which
263 generates low internal tensile stress in the gel phase. Hence the orientation degree decreases.
264 However, at the end (close to the center of the gel), birefringence decreases sharply. We
265 considered that at the central part of the gel, the collagen molecules are subjected to tensile
266 stress from all directions, which leads to the formation of poorly oriented structure.



267
 268 **Figure 4 (a)** POM images (crossed polarizer both in absence and presence of tint plate) of
 269 SBC hydrogels (1 hour gelation) prepared at 25°C having concentration ranges from 1.2 wt%
 270 to 4 wt%. Illustration of orientation structure of SBC identified by POM is shown on the right
 271 side of POM images. A: analyzer, P: polarizer, X' and Z': fast and slow axes of the tint plate,
 272 respectively. All the POM images are in same scale as shown in the top left part. **(b)** The
 273 birefringence variation of SBC hydrogel (2 hours gelation), with the distance from periphery
 274 to center (l) of the hydrogel.

275
 276 Diffusion induced superstructure formation in SBC hydrogel is quite similar to our previous
 277 study,³⁷ where the binding of negatively charged PBDT molecule with Ca^{2+} ion creates ring
 278 shaped concentric orientation pattern. According to our knowledge, it is the first success in
 279 creating concentric ring pattern macroscopic superstructure in collagen hydrogel by diffusion
 280 induced gelation. Attempt by Furusawa *et al.*²² demonstrated that, diffusion of buffer through
 281 the type I bovine dermis collagen solution made phase separated tubular pores aligned
 282 parallel to the growth direction of the gel. This result suggests that different sources of
 283 collagen have big impact for the creation of oriented structure. So we further performed
 284 diffusion induced gelation in some traditionally used animal collagens as control experiment.
 285 For this purpose, we used calf skin collagen (CSC) in tropocollagen form and porcine skin
 286 collagen (PSC) in atelocollagen form. We found that both CSC and PSC only form very weak,

287 non-self-standing gels. Figure 5 shows the POM images of 2 wt% CSC and PSC samples
 288 prepared at 25°C and 34°C. The samples prepared at 34°C are more turbid than that prepared
 289 at 25°C (Figure 5), which indicates that these collagens have better fibrillogenesis capacity at
 290 higher temperature. Interestingly, no birefringence is observed in all cases, except a thin weak
 291 concentric birefringence at the periphery of PSC gel prepared at 34°C, indicating that almost
 292 random structure is formed in both CSC and PSC hydrogel.



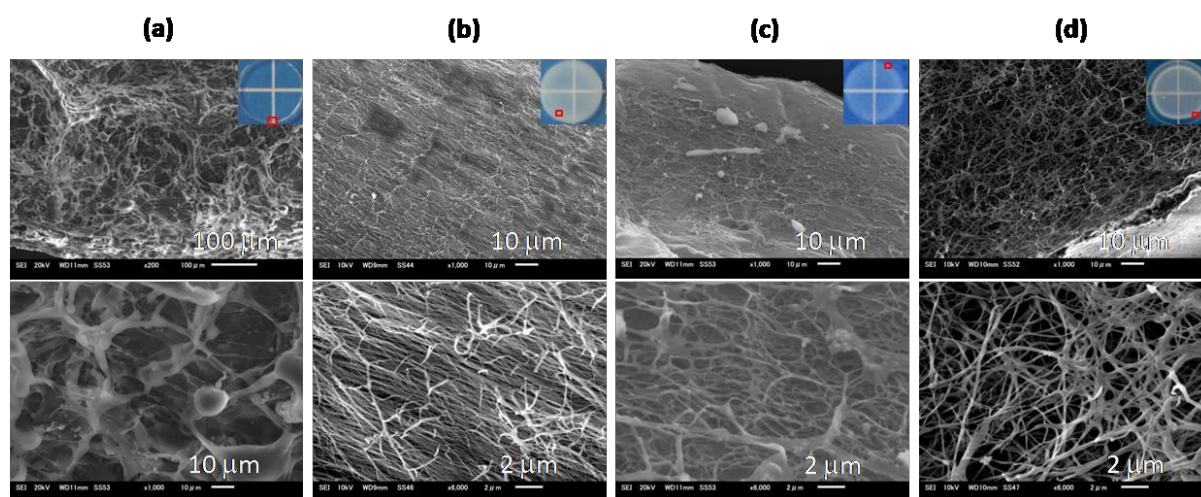
293

294

295 **Figure 5** The photographs (I) and POM images (II, III) of (a) 2 wt% calf skin collagen (CSC)
 296 hydrogel and (b) 2 wt% porcine skin collagen (PSC) hydrogel prepared by 3 hours gelation at
 297 25°C and 34°C. Illustrations (IV) of orientation patterns of collagen identified by POM are
 298 shown on the right side of POM images. A: analyzer, P: polarizer, X' and Z': fast and slow
 299 axes of the tint plate, respectively. All the images are in same scale as shown in the top left
 300 part.

301

302 We have also confirmed orientation and morphology of fibril structure through SEM
 303 observation. Figure 6 (a) and (b) show the SEM images of 4 wt% SBC solution and hydrogel,
 304 respectively. All the samples were fixed by glutaraldehyde before performing SEM. SBC
 305 solution does not contain any fibril, rather it makes cluster of network polymer (Figure 6(a)),
 306 may be formed by glutaraldehyde crosslinking process. SBC hydrogel made by reaction-
 307 diffusion (RD) process contains solely of collagen fibrils, which are beautifully aligned
 308 perpendicular to the diffusion direction with an almost homogeneous fibril diameter of ~200
 309 nm (Figure 6(b)). On the other hand, both CSC (Figure 6(c)) and PSC (Figure 6(d)) gels
 310 contain randomly oriented collagen fibril with inhomogeneous distribution of fibril size.



311

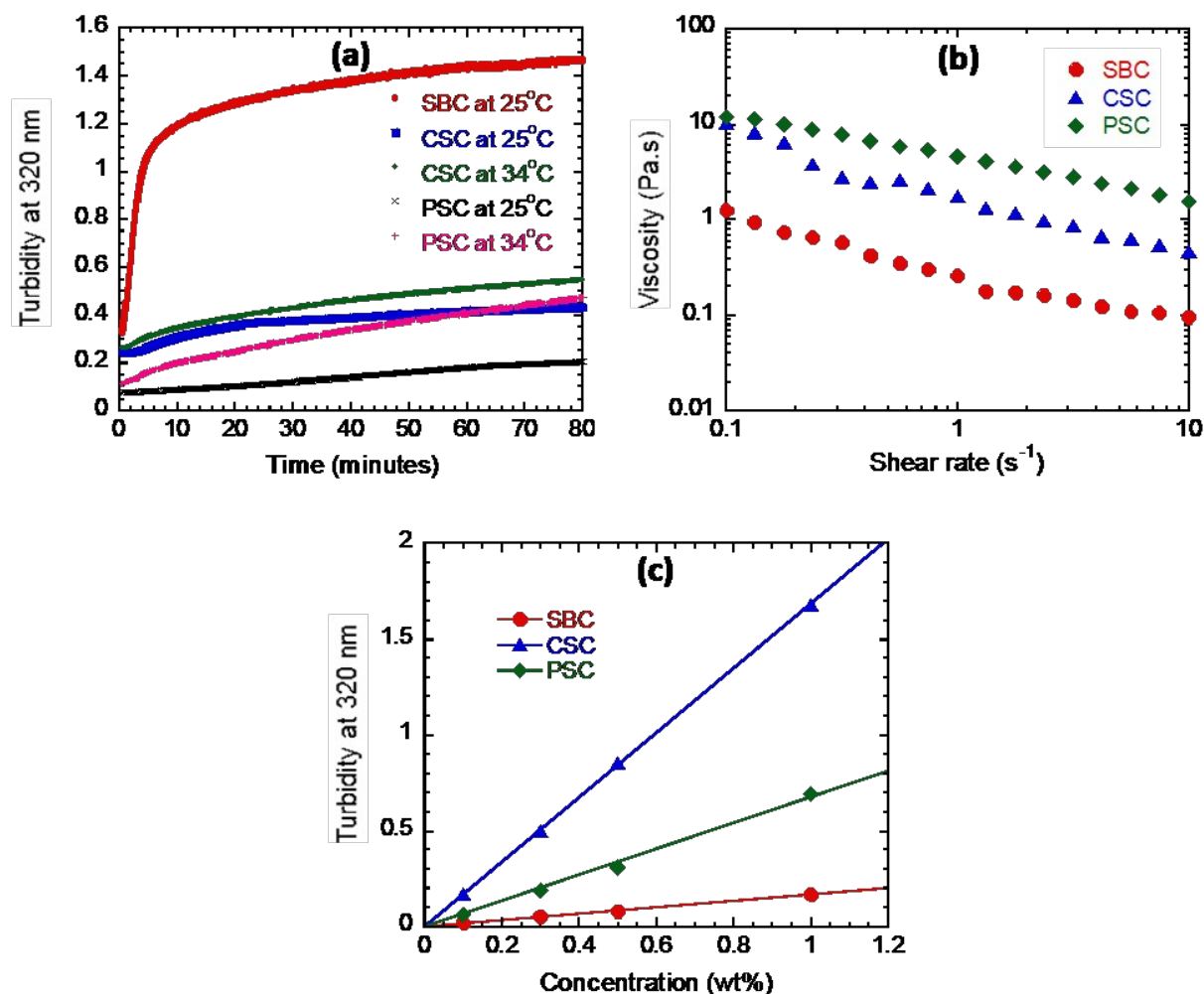
312

313 **Figure 6** SEM images of (a) 4 wt% SBC solution, (b) 4 wt% SBC gel prepared at 25°C, (c) 2
 314 wt% CSC gel prepared at 34°C, (d) 2 wt% PSC gel prepared at 34°C. The red rectangular
 315 markers in onset samples' photographs indicate the observation region of SEM images.
 316 Lower row images are the magnified images of the corresponding upper row images.

317

318 One of the most important criteria we assumed, to develop internal stress from swelling
 319 mismatch in the RD process, is the *fast rate of bundle formation* among the rigid
 320 macromolecules with diffusing ions. Quick bundle formation causes large swelling mismatch

321 at the gel/sol phase boundary by solvent squeezing and therefore, can develop internal stress
322 large enough to cause alignment of the rigid macromolecules along the gelation front line,
323 which is frozen instantly to give the anisotropic structure. This may explain why, the
324 fibrillogenesis rate of collagen in buffer solution must be very high to ensure the formation of
325 aggregated structure by diffusion process and develop enough internal stress to create
326 oriented structure. In the case of most of the conventional animal collagen, fibrillogenesis
327 rate is very slow.^{17,43,44} Zhang *et al.*¹⁷ reported that, the fibrillogenesis rate of porcine tendon
328 collagen is very slow compared to SBC. Figure 7(a) shows the comparative fibrillogenesis
329 rate for SBC, CSC and PSC. At the present experimental conditions, fibrillogenesis rate of
330 both animal collagens (CSC and PSC) is very slow, which ultimately causes the failure of
331 creating oriented structure in CSC and PSC gels by diffusion induced gelation process.
332 However, the fibrillogenesis rate of animal collagens (CSC and PSC) increases a bit at 34°C;
333 but may be, still far away from the required quantity of gelation rate for the creation of
334 ordered structure.



335

336 **Figure 7 (a)** Turbidity changes at 320 nm of an equal volume mixture of 0.3 wt% collagen
 337 solution and 0.1 M Na-phosphate buffer (pH 7.2). The abrupt increase of turbidity of SBC
 338 indicates its fast rate of *in vitro* fibril formation in the neutral buffer in comparison to CSC
 339 and PSC. **(b)** The variation of dynamic viscosity (at 25°C) of acidic SBC, CSC and PSC
 340 solutions with the shear rate ranges from 0.1 s⁻¹ to 10 s⁻¹. **(c)** The concentration dependence of
 341 turbidity at 320 nm (25°C) for acidic SBC, CSC and PSC solutions. The high turbidity of
 342 CSC and PSC indicates the occurrence of fibril formation in comparison to SBC.

343

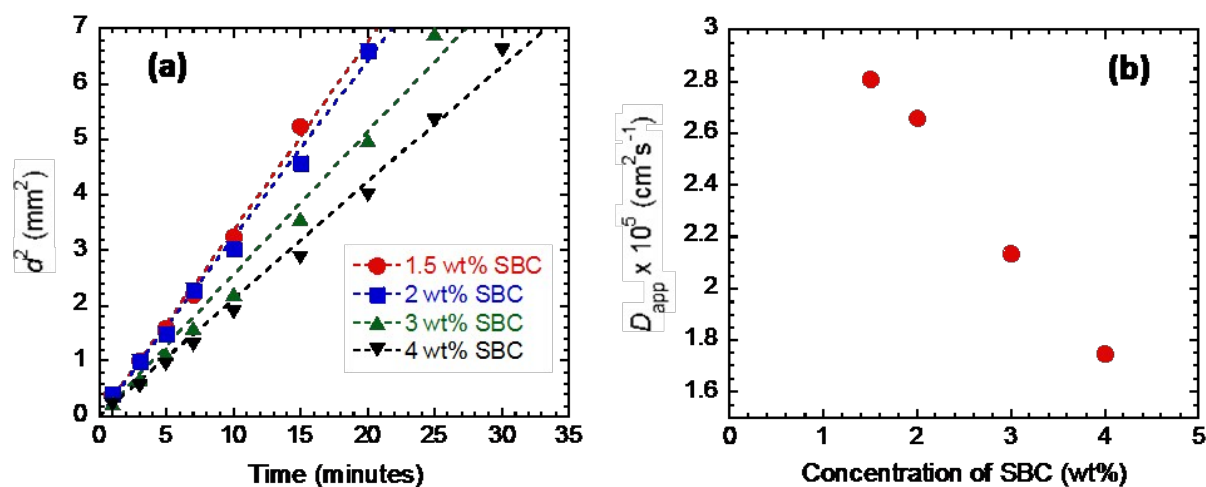
344 Additionally, the viscosity of animal collagens (CSC and PSC) in acidic solution increases
 345 very rapidly with concentration, and above 2 wt% concentration, it becomes very difficult to
 346 handle. For example, the viscosity of 1wt% CSC at 0.1 s⁻¹ is 10.14 Pa.s and 1wt% PSC is

347 12.05 Pa.s, which are about one order higher than that of SBC (1.25 Pa.s) (Figure 7(b)). The
348 high viscosity of the CSC and PSC in acidic solution is due to the formation of aggregated
349 structure, as shown by the dramatic increase of turbidity of animal collagens at high
350 concentration (Figure 7(c)). We speculated that these aggregated structures make it difficult
351 to form oriented structure of collagen by swelling mismatching. In contrast, SBC solution has
352 much lower viscosity and turbidity than CSC and PSC. This makes it possible to perform the
353 controlled gelation of SBC at high concentration (4 wt%), close to the native tissues. In
354 summary, fast fibrillogenesis rate, high solubility and homogeneity, and low viscosity causes
355 extremely high degree of fiber formation, which makes the SBC very special for forming
356 hydrogels with ordered structure.

357

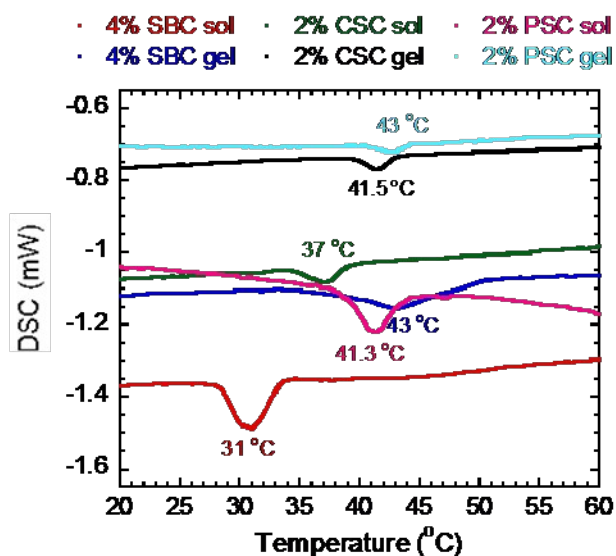
358 To get better understanding about the diffusion process, we quantitatively studied the
359 diffusion features. The small ions of neutral phosphate buffer (HPO_4^{2-} , H_2PO_4^- , Na^+) diffuse
360 through the SBC solution and induce gelation. Since the fibrillogenesis rate of SBC is
361 extremely fast and the translational motion of large triple-helix collagen molecule is very
362 slow compared to the small buffer ions, it is expected that the gelation of SBC would be
363 mostly controlled by the diffusion of buffer solution. This is confirmed by the linear
364 relationship between the square of the gel layer width (distance between the periphery and the
365 gelation front), d^2 and the gelation time, t for different concentrations of SBC as shown in
366 Figure 8(a). The apparent diffusion coefficient, D_{app} of 0.1 M Na-phosphate buffer (pH 7.2) is
367 calculated from Figure 8(a) using the relationship, $d^2 = 2D_{\text{app}}t^{45}$ and plotted against the
368 concentrations of SBC in Figure 8(b). The values of D_{app} are in the same order with the
369 diffusion constant of small ions in water ($D_0(\text{HPO}_4^{2-}) = 1.49 \times 10^{-5} \text{ cm}^2\text{s}^{-1}$, $D_0(\text{H}_2\text{PO}_4^-) = 1.03$
370 $\times 10^{-5} \text{ cm}^2\text{s}^{-1}$, $D_0(\text{Na}^+) = 2.53 \times 10^{-5} \text{ cm}^2\text{s}^{-1}$; calculated by using Stokes-Einstein equation⁴⁶),
371 and decrease linearly with increasing the concentrations of SBC. As the concentrations of

372 SBC increases, more buffer ions are consumed to induce fibrillogenesis and therefore, the
 373 D_{app} decreases.



374
 375 **Figure 8 (a)** Relationship between the square of the gel layer width (d^2) and gelation time (t)
 376 for SBC hydrogels of various concentrations. **(b)** The change in apparent diffusion
 377 coefficient, D_{app} (calculated from the slopes of (a) using the relationship, $d^2 = 2D_{app}t$) of 0.1
 378 M Na-phosphate buffer (pH 7.2) with the concentrations of SBC.

379
 380 The differential scanning calorimetry (DSC) experiments (Figure 9) show that the
 381 denaturation temperature (T_d) of SBC hydrogel rises significantly from 31°C (32.9°C by CD
 382 spectroscopy¹⁷) to 43°C after the gelation, indicating the formation of thick stable fiber by
 383 diffusion induced gelation process. However in the case of CSC, T_d raises little from 37°C to
 384 41°C, indicating that the further aggregation by buffer diffusion from the initial turbid
 385 solution is not so high. Similar result was observed in PSC gel. Therefore, the samples
 386 obtained from both CSC and PSC (at 25°C) was very weak and it broken into fragments when
 387 we removed the cover glass of the reaction cell. On the contrary, SBC form strong gel that
 388 could be handled easily.

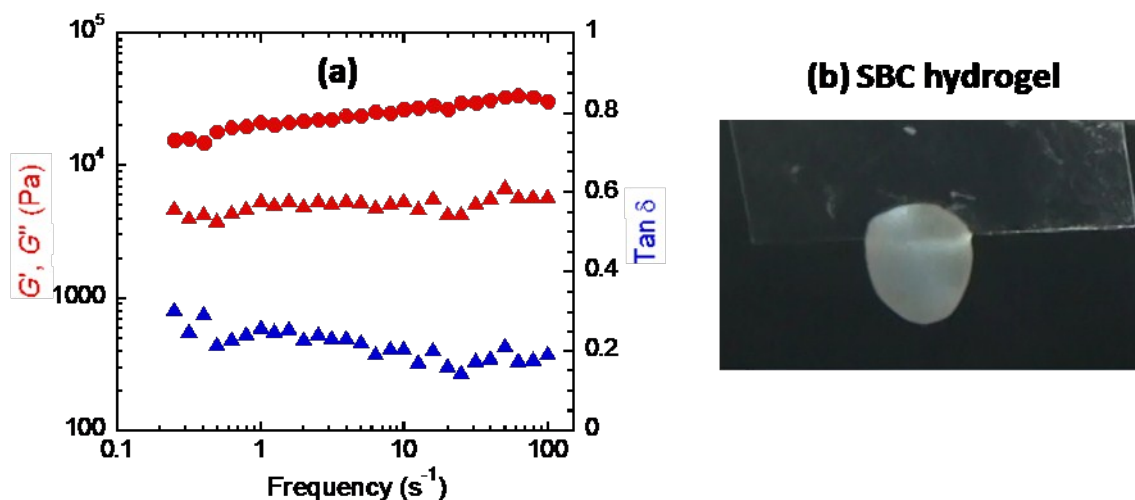


389

390 **Figure 9** DSC curves of SBC, CSC and PSC (both solution and hydrogel) heated at 1°C/min.

391

392 To characterize the mechanical strength of SBC hydrogel we have measured dynamic
 393 modulus by applying torsion along the collagen orientation direction. The dynamic frequency
 394 sweep test of 4 wt% SBC hydrogel at a constant strain of 0.2% is shown in Figure 10(a). The
 395 SBC hydrogel shows a storage modulus about 15-30 kPa, which increases slightly with
 396 frequency. The loss tangent is around 0.2. These results confirm that the SBC forms a soft
 397 and elastic hydrogel. Figure 10(b) demonstrated that SBC gel can hang freely from the edge
 398 of glass plate without any damage, indicating its self-standing ability. We found that the
 399 mechanical strength and T_d value of SBC gel can be increased further by using chemical
 400 cross-linker (data not shown). Since the strength of this 3D gel is sufficiently high and T_d
 401 value (43°C) is well above the physiological temperature, this material would be suitable for
 402 cell culture and other biomedical applications.



403
 404 **Figure 10** (a) Frequency dependence of the storage modulus (G' - red circle), loss modulus
 405 (G'' - red triangle), and loss tangent ($\tan \delta$ - blue triangle) of 4 wt% SBC gel at 25°C and a
 406 constant strain amplitude of 0.2%. (b) Free hanging of 4 wt% SBC hydrogel from the edge of
 407 glass without any damage indicates its self-standing ability.

408

409 4. CONCLUSIONS

410 Disk shaped physical hydrogels with concentric orientation of collagen fibrils are prepared
 411 from swim bladder collagen (SBC) of Bester sturgeon fish using a facile experimental
 412 method. SBC meets all the criteria to form oriented and self-standing hydrogel by diffusion
 413 induced gelation process. However, calf skin collagen (CSC) and porcine skin collagen (PSC)
 414 could not form any oriented structure. The high aggregated structure, slow fibrillogenesis
 415 rate, high viscosity and less homogeneity at high concentrations of animal collagens are not
 416 favorable to form ordered structure by reaction-diffusion (RD) method. On the other hand,
 417 the less aggregated structure, fast fibrillogenesis rate, and low viscosity of SBC solution favor
 418 oriented superstructure formation by the controlled diffusion of buffer. Swelling mismatch
 419 between the gel phase and the sol phase due to the quick solvent squeezing by fast
 420 fibrillogenesis process (*syneresis effect*), generates an internal tensile stress in the collagen
 421 molecules of gel phase, which assist them to align along the gel-sol interface direction to give

422 concentric ring-shaped orientation pattern. An anisotropic orientation gradient from periphery
423 to center has been formed due to the change in diffusion velocity in respective regions. The
424 denaturation temperature (T_d) of SBC hydrogel rises significantly from 31°C of SBC solution
425 to 43°C due to its excellent fiber forming capacity, however; T_d of both CSC and PSC gels
426 increase a little from that of their solutions. SBC gel has reasonably high mechanical strength
427 (storage modulus > 15 kPa). This SBC hydrogel made from marine-based atelocollagen,
428 having macroscopic superstructure, self-standing capability and high thermal stability, will be
429 suitable for cell culture and other biological applications. Our study would help to understand
430 the mechanism and requirements for creating anisotropic hydrogel by RD method.
431 Controlling the diffusion process of neutral buffer solution through SBC solution might be
432 able to create different orientation pattern in SBC hydrogel, which offers further opportunity
433 for functionalization of collagen hydrogel. SBC seems to have bright prospect for creating
434 next generation artificial bio-materials.

435

436 5. REFERENCES

- 437 (1) J. P. Gong, Y. Katsuyama, T. Kurokawa and Y. Osada, *Adv. Mater.*, 2003, **15**, 1155-1158.
- 438 (2) M. A. Haque, G. Kamita, T. Kurokawa, K. Tsujii and J. P. Gong, *Adv. Mater.*, 2010, **22**,
439 5110–5114.
- 440 (3) J. Y. Sun, X. Zhao, W. R. K. Illeperuma, O. Chaudhuri, K. H. Oh, D. j. Mooney, J. J.
441 Vlassak and Z. Suo, *Nature*, 2012, **489**, 133–136.
- 442 (4) T. L. Sun, T. Kurokawa, S. Kuroda, A. B. Ihsan, T. Akasaki, K. Sato, M. A. Haque, T.
443 Nakajima and J. P. Gong, *Nat. Mater.*, 2013, **12**, 932–937.
- 444 (5) R. Takahashi, Z. L. Wu, M. Arifuzzaman, T. Nonoyama, T. Nakajima, T. Kurokawa and
445 J. P. Gong, *Nat. Commun.*, 2014, **5**, 4490.

- 446 (6) A. R. Liberski, J. T. Delaney, H. Schafer, J. Perelaer and U. S. Schubert, *Macromol.*
447 *Biosci.*, 2011, **11**, 1491–1498.
- 448 (7) A. S. Hoffman, *Adv. Drug Delivery Rev.*, 2012, **64**, 18–23.
- 449 (8) B. V. Slaughter, S. S. Khurshid, O. Z. Fisher, A. Khademhosseini and N. A. Peppas, *Adv.*
450 *Mater.*, 2009, **21**, 3307–3329.
- 451 (9) Y. Qiu and K. Park, *Adv. Drug Delivery Rev.*, 2012, **64**, 49–60.
- 452 (10) L. Cen, W. Liu, L. Cui, W. Zhang and Y. Cao, *Pediatr. Res.*, 2008, **63**, 492–496.
- 453 (11) R. Parenteau-Bareil, R. Gauvin and Berthod, F. *Materials*, 2010, **3**, 1863–1887.
- 454 (12) S. Weiner and H. D. Wagner, *Annu. Rev. Mater. Sci.*, 1998, **28**, 271–298.
- 455 (13) C. Sanchez, H. Arribart and M. M. Giraud-Guille, *Nat. Mater.*, 2005, **4**, 277–288.
- 456 (14) A. Jongjareonrak, S. Benjakul, W. Visessanguan, T. Nagai and M. Tanaka, *Food Chem.*,
457 2005, **93**, 475–484.
- 458 (15) F. Zhang, A. Wang, Z. Li, S. He and L. Shao, *Food Nutr. Sci.*, 2011, **2**, 818–823.
- 459 (16) S. Yamada, K. Yamamoto, T. Ikeda, K. Yanagiguchi and Y. Hayashi, *BioMed Res. Int.*,
460 2014, **2014**, 1–8.
- 461 (17) X. Zhang, M. Ookawa, Y. Tan, K. Ura, S. Adachi and Y. Takagi, *Food Chem.*, 2014,
462 **160**, 305–312.
- 463 (18) T. Nagai and N. Suzuki, *Food Chem.*, 2000, **68**, 277–281.
- 464 (19) F. Pati, B. Adhikari and S. Dhara, *Bioresour. Technol.*, 2010, **101**, 3737–3742.
- 465 (20) A. Sanoa, M. Maedaa, S. Nagaharaa, T. Ochiyab, K. Honmac, H. Itohc, T. Miyatac and
466 K. Fujiokaa, *Adv. Drug Delivery Rev.*, 2003, **55**, 1651–1677.
- 467 (21) W. Friess, *Eur. J. Pharm. Biopharm.*, 1998, **45**, 113–136.
- 468 (22) K. Furusawa, S. Sato, J. Masumoto, Y. Hanazaki, Y. Maki, T. Dobashi, T. Yamamoto,
469 A. Fukui and N. Sasaki, *Biomacromolecules*, 2012, **13**, 29–39.
- 470 (23) N. Saeidi, E. A. Sander and J. W. Ruberti, *Biomaterials*, 2009, **30**, 6581–6592.

- 471 (24) P. Lee, R. Lin, J. Moon and L. P. Lee, *Biomed. Microdevices*, 2006, **8**, 35–41.
- 472 (25) F. Jiang, H. Horber, J. Howard and D. J. Muller, *J. Struct. Biol.*, 2004, **148**, 268–278.
- 473 (26) X. Cheng, U. A. Gurkan, C. J. Dehen, M. P. Tate, H. W. Hillhouse, G. J. Simpson and
474 O. Akkus, *Biomaterials*, 2008, **29**, 3278–3288.
- 475 (27) J. A. Matthews, G. E. Wnek, D. G. Simpson and G. L. Bowlin, *Biomacromolecules*,
476 2002, **3**, 232-238.
- 477 (28) C. Guo and L. J. Kaufman, *Biomaterials*, 2007, **28**, 1105–1114.
- 478 (29) J. Torbet, M. Malbouyres, N. Builles, V. Justin, M. Roulet, O. Damour, A. Oldberg, F.
479 Ruggiero and Hulmes, D.J.S. *Biomaterials*, 2007, **28**, 4268–4276.
- 480 (30) R. M. Capito, H. S. Azevedo, Y. S. Velichko, A. Mata and S. I. Stupp, *Science*, 2008,
481 **319**, 1812-1816.
- 482 (31) K. Furusawa, Y. Minamisawa, T. Dobashi and T. Yamamoto, *J. Phys. Chem. B*, 2007,
483 **111**, 14423-14430.
- 484 (32) Y. Maki, K. Ito, N. Hosoya, C. Yoneyama, K. Furusawa, T. Yamamoto, T. Dobashi, Y.
485 Sugimoto and K. Wakabayashi *Biomacromolecules*, 2011, **12**, 2145-2152.
- 486 (33) T. Dobashi, K. Furusawa, E. Kita, Y. Minamisawa and T. Yamamoto, *Langmuir*, 2007,
487 **23**, 1303-1306.
- 488 (34) W. Yang, H. Furukawa and J. P. Gong, *Adv. Mater.*, 2008, **20**, 4499-4503.
- 489 (35) Z. L. Wu, T. Kurokawa, D. Sawada, J. Hu, H. Furukawa and J. P. Gong,
490 *Macromolecules*, 2011, **44**, 3535-3541.
- 491 (36) Z. L. Wu, T. Kurokawa and J. P. Gong, *Polym. J.*, 2012, **44**, 503–511.
- 492 (37) Z. L. Wu, R. Takahashi, D. Sawada, M. Arifuzzaman, T. Nakajima, T. Kurokawa, J. Hu
493 and J. P. Gong, *Macromolecules*, 2014, **47**, 7208–7214.
- 494 (38) J. A. Uquillas and O. Akkus, *Ann. Biomed. Eng.*, 2012, **40**, 1641-1653.

- 495 (39) Y. Li, A. Asadi, M. R. Monroe and E. P. Douglas, *Mater. Sci. Eng., C*, 2009, **29**, 1643-
496 1649.
- 497 (40) M. M. Giraud-Guille, *Biol. Cell*, 1989, **67**, 97–101.
- 498 (41) F. Gobeaux, E. Belamie, G. Mosser, P. Davidson, P. Panine and M. M. Giraud-Guille,
499 *Langmuir*, 2007, **23**, 6411-6417.
- 500 (42) M. Wolman and F.H. Kasten, *Histochemistry*, 1986, **85**, 41-49.
- 501 (43) B. R. Williams,; R. A. Gelman, D. C. Poppke and K. A. Piez, *J. Biol. Chem.*, 1978, **253**,
502 6578-6585.
- 503 (44) G. C. Na, L. J. Butz and R. J. Carroll, *J. Biol. Chem.*, 1986, **261**, 12290-12299.
- 504 (45) A. Einstein, *Investigations on the Theory of Brownian Movement*; Dover: New York,
505 1926.
- 506 (46) A. Einstein, *Annalen der Physik*, 1905, **17**, 549.
- 507
- 508
- 509
- 510
- 511
- 512
- 513
- 514
- 515
- 516
- 517
- 518
- 519

520 **Graphical abstract**

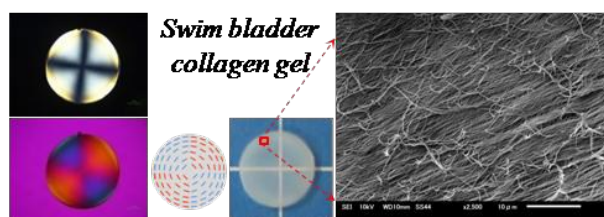
521

522 **Swim bladder collagen forms hydrogel with macroscopic superstructure by**
523 **diffusion induced fast gelation**524 Md. Tariful Islam Mredha^a, Xi Zhang^b, Takayuki Nonoyama^c, Tasuku Nakajima^c, Takayuki
525 Kurokawa^c, Yasuaki Takagi^d and Jian Ping Gong^{c*}526 ^a*Graduate School of Life Science, Hokkaido University, Sapporo 060-0810, Japan*527 ^b*Graduate School of Fisheries Sciences, Hokkaido University, Hakodate 041-8611, Japan*528 ^c*Faculty of Advanced Life Science, Hokkaido University, Sapporo 060-0810, Japan*529 ^d*Faculty of Fisheries Sciences, Hokkaido University, Hakodate 041-8611, Japan*530 **Corresponding author-*531 *E-mail: gong@mail.sci.hokudai.ac.jp (J.P.G); Tel & FAX: +81-(0)11-706-2774*

532

533

534



535

536

537

538 **Highlights**539 Type I collagen extracted from swim bladder of Bester sturgeon forms oriented hydrogel with
540 mechanical and thermal stability by diffusion induced fast gelation.